Quantum Electronics **50** (7) 653–657 (2020)

https://doi.org/10.1070/QEL17294

Bragg grating inscription in photosensitive materials by an optical replication process

S.B. Odinokov, A.Yu. Zherdev, M.V. Shishova, A.B. Solomashenko, D.S. Lushnikov, V.V. Markin

Abstract. **This paper examines the feasibility of producing multiplexed Bragg gratings for use as diffractive optical elements (DOEs) by coherent optical replication of a surface-relief phase grating into thick-film photosensitive materials. The use of such DOEs in light guide plates (LGPs) for optical imaging systems ensures energy-efficient light input into and output from LGPs and allows one to minimise their weight and size. We present simulation results for the interference structure fabrication process and recording of a series of multiplexed diffraction gratings in photosensitive materials.**

Keywords: *optical replication, interference copying, holographic and diffractive optical elements, Bragg gratings.*

1. Introduction

At present, to minimise the weight and size of the optical systems of augmented reality devices and visual instruments (telescopes and sighting devices) and those of 3D screens, active use is made of light guide plates (LGPs) with diffractive optical elements (DOEs) [1, 2]. In most cases, a system of several 'thin' surface-relief phase gratings is produced in such plates with DOEs on their surface, and the gratings serve to couple (mono- or polychromatic) light into and outcouple it from a glass plate of certain thickness in which the light propagates under total internal reflection (TIR) conditions [3]. DOEs are, in turn, made in the form of a structure of diffraction gratings, which match incident and emerging collimated light beams to their propagation in the glass LGP, thus allowing one to produce 'planar' optical components with as small a weight and size as possible [4]. However, 'thin' surface-relief phase gratings have low diffraction efficiency (in practice, no higher than 15%–20% [5]) and fail to ensure the required range of angles (above 25°) for coupling collimated optical radiation (light) beams into and outcoupling them from LGPs. Moreover, in producing colour images in optical radiation incoupling and outcoupling devices at different wavelengths, use is made of three layers of 'thin' surface-relief phase gratings in order to redirect light of different wavelengths (spectral components) at required angles. In doing so, the parameters of each layer of such 'thin' surface-relief phase gratings should be additionally optimised for the corresponding wavelength, which significantly complicates the grating inscription process.

Diffraction efficiency of optical systems can be improved by a factor of 2–3 by using Bragg gratings [6] written into thick-film photosensitive materials, and the optical radiation incoupling/outcoupling field angles can be increased by raising the spatial frequency of the diffraction gratings to 2500–3000 lines per millimetre and choosing an appropriate angular selectivity for them. In such a case, multiplexed Bragg grating writing (up to 20–30 multiplexes) should be performed in thick-film photosensitive materials.

Thus, the use of Bragg gratings is a logical step in creating a new generation of DOEs for light guide plates, e.g. in the optical systems of augmented reality devices. If Bragg gratings are used, the angular and spectral selectivities of the multiplexed grating should be optimised for their part of the angular field upon the incoupling and outcoupling of collimated light beams [7]. Such a representation is sort of an analogue of a 'holographic Bragg mirror' cascade. Bragg gratings are traditionally used to produce optical radiation beams with high angular selectivity (angle standard) or spectral selectivity (spectral filter for semiconductor and fibre lasers). If Bragg gratings are used as DOEs for light guides in optical schemes of devices, e.g. of augmented reality devices, there are opposite requirements: angular and spectral selectivities should be as low as possible in order to produce less multiplexes. In such a case, the function of Bragg gratings is to redirect collimated light beams in concert with waveguide propagation in a glass LGP and required beam outcoupling angles.

In this paper, we propose a method for optical replication of a 'thin' surface-relief phase grating (hereafter photomask) in coherent light for multiplexed Bragg grating inscription (up to 50 multiplexes) in thick-film photosensitive materials. This replication method allows one to significantly simplify the optical scheme for recording multiplexed Bragg gratings to be used as DOEs for light guide plates because it does without the standard cumbersome scheme involving interference of two coherent light beams, which requires serious vibration isolation in the case of prolonged exposures and the fabrication of high-frequency Bragg gratings (up to 3000 lines per millimetre). Moreover, in the case of coherent optical replication, use is made not of three expensive 'colour' lasers (for producing 'colour' DOEs in the RGB representation) but of one laser with a wavelength determined by the spectral sensitivity of photomaterials. The method allows these complex optical schemes to be replaced by a significantly simpler one, using a series of appropriate photomasks in the form of one or a set of a few 'thin' surface-relief phase gratings. The fabrication of such gratings on photoresist layers by laser and elec-

S.B. Odinokov, A.Yu. Zherdev, M.V. Shishova, A.B. Solomashenko, D.S. Lushnikov, V.V. Markin Bauman Moscow State Technical University (National Research University), Vtoraya Baumanskaya ul. 5/1, 105005 Moscow, Russia; e-mail: mshishova@bmstu.ru

Received 18 February 2020; revision received 19 March 2020
Kvantovaya Elektronika **50** (7) 653–657 (2020)
Translated by O.M. Tsarev

tron beam lithography techniques was worked out long ago [8]. In addition, the method allows a structure of three 'thin' surface-relief phase gratings (for producing RGB colour images) to be replaced by one multiplexed Bragg grating structure produced in one photosensitive material. As a result, one can obtain a single optical component with improved energy efficiency and an increased angle of the field of the collimated light beams emerging from the LGP, which ensures considerably more stable performance parameters of the light guide plate with DOEs in the optical systems of devices and instruments. The use of thick-film photosensitive materials such as photothermorefractive glass (up to several millimetres in thickness [9]), which is completely free of shrinkage effects, maximises the stability of all parameters and characteristics of Bragg gratings.

2. Simulation of the interference structure fabrication process

The simulation of the fabrication of multiplexed Bragg gratings written as input and output diffraction gratings by optical replication [10], to be subsequently used for producing a single light guide plate with DOEs, included the use of a series of photomasks in the form of surface-relief phase gratings with required spatial frequencies. As shown in Fig. 1, the following physical processes underlie this method of optical replication of a 'thin' surface-relief phase grating into a thick-film photosensitive material (bulk medium). In the near field of the Fresnel diffraction region, interference of diffracted optical radiation occurs between the beams of the 0, +1 and –1 orders. In the English language literature, an analogous process is referred to as single-exposure interference lithography, or holographic lithography, with a template (or phase mask) [11, 12]. It is often employed to record gratings in photonic crystals – in both photoresist [13] and bulk media [14].

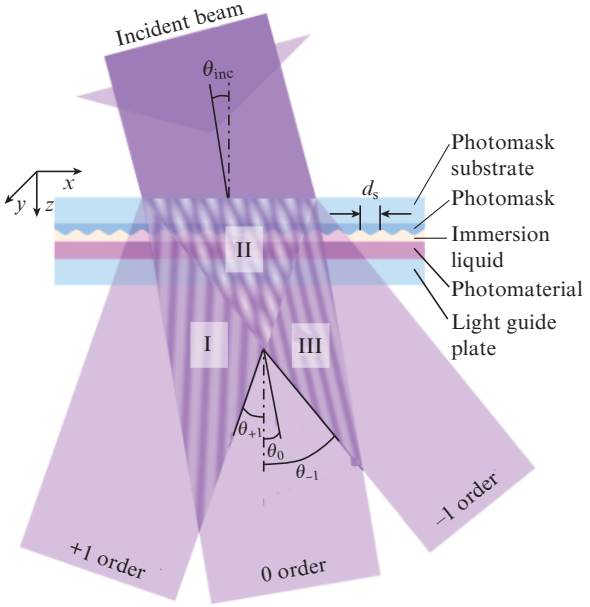

Figure 1. Schematic illustrating the formation of interfering coherent light beams in regions I–III during Bragg grating inscription in a photosensitive material by the proposed replication method: θ_{inc} is the angle of incidence of the beam, θ_m ($m = 0, +1, -1$) is the angle of the diffracted beam of the mth order, and d_s is the grating period.

This optical replication method allows one to ensure high spatial frequencies of Bragg gratings, which are also referred to as strata after recording in a photomaterial [9, 10, 12]. An additional advantage of the method is that, during Bragg grating multiplexing, in each subsequent exposure it is necessary to merely tilt the sample with a template in the writing beam, which significantly simplifies the process. Recording is performed with coherent monochromatic light actinic for a particular thick-film photosensitive material [dichromated gelatin (DCG) and photopolymers]. In addition, the method allows one to record Bragg gratings (as 3D structures) with a period considerably smaller than the photomask period. For copying, the emulsion sides of the photosensitive material and template ('thin' surface-relief phase grating) should be joined through an immersion liquid to avoid spurious interference fringes.

It is seen from Fig. 1 that, if a 'thin' surface-relief phase grating with period d_s is used as a template, three orders of diffraction are formed in the photosensitive material according to the grating equation. The incident beam diameter should correspond to the size of the recording region. Thus, if use is made of optical radiation with a wavelength λ lying in the spectral sensitivity region of the photomaterial, there are three recording regions: region II, where the beams of all three diffraction orders (0, +1 and –1 orders) interfere, and regions I and III, where only the 0 and +1 orders and the 0 and –1 orders interfere, respectively. Interference of the 0 and –1 orders in region III and that of the 0 and +1 orders in region I can be interpreted as the formation of working directions of constant-phase planes in the final structure of Bragg gratings, which become strata (holographic mirrors) after recording in a photomaterial.

To analyse a structure being recorded, we simulate the interference process. Let the complex amplitudes of interfering waves have the form $\boldsymbol{E}_1\exp(-\mathrm{j}\boldsymbol{k}_1\boldsymbol{r})$, $\boldsymbol{E}_2\exp(-\mathrm{j}\boldsymbol{k}_2\boldsymbol{r})$ and $\boldsymbol{E}_3\exp(-\mathrm{j}\boldsymbol{k}_3\boldsymbol{r})$, which corresponds to the above three orders of diffraction. Then as a result of the interference of these waves in regions I–III we obtain the light intensity distribution

$$I(\boldsymbol{r}) = |\boldsymbol{E}_\Sigma(\boldsymbol{r})|^2 = \left|\sum_{n=1}^{3}\boldsymbol{E}_n\exp(-\mathrm{j}\boldsymbol{k}_n\boldsymbol{r})\right|^2$$

$$= I_0\left[\sum_{i=1}^{2}\sum_{j=i+1}^{3}V_{ij}\cos(\boldsymbol{K}_{ij}\boldsymbol{r}+\varphi_{ij})\right], \quad (1)$$

where $I_0 = \sum_{n=1}^{N}|\boldsymbol{E}_n|^2$ is the total light intensity; $V_{ij} = |\boldsymbol{E}_i\boldsymbol{E}_j|/I_0$ is the contrast of the interference fringe between the ith and jth beams; $\boldsymbol{K}_{ij} = \boldsymbol{k}_i - \boldsymbol{k}_j$ is the grating vector for interference between the ith and jth beams; the wave vectors $\boldsymbol{k}_N$ are determined by diffraction angles; and φ_{ij} is the phase difference between the ith and jth beams. Each pair of interfering beams produces one sinusoidal grating, which is characterised by vector $\boldsymbol{K}_{ij}$. The simulation results for a single-exposure process (without sequential multiplexing) are presented in Fig. 2.

As a result, there are four stratum directions, determined by the angle of incidence of the light (illumination) on the photomask, and the 'working' direction, ensuring adequate operation at a particular wavelength, is normal to vector $\boldsymbol{K}_2$ (Fig. 2). It is for a Bragg grating with vector $\boldsymbol{K}_2$ that parameters of the template and the recording angle are first calculated in order to separate the other gratings, with vectors $\boldsymbol{K}_1$, $\boldsymbol{K}_3$ and $\boldsymbol{K}_4$, which are actually 'noise' ('parasitic') directions, producing so-called parasitic gratings, not involved in resolv-

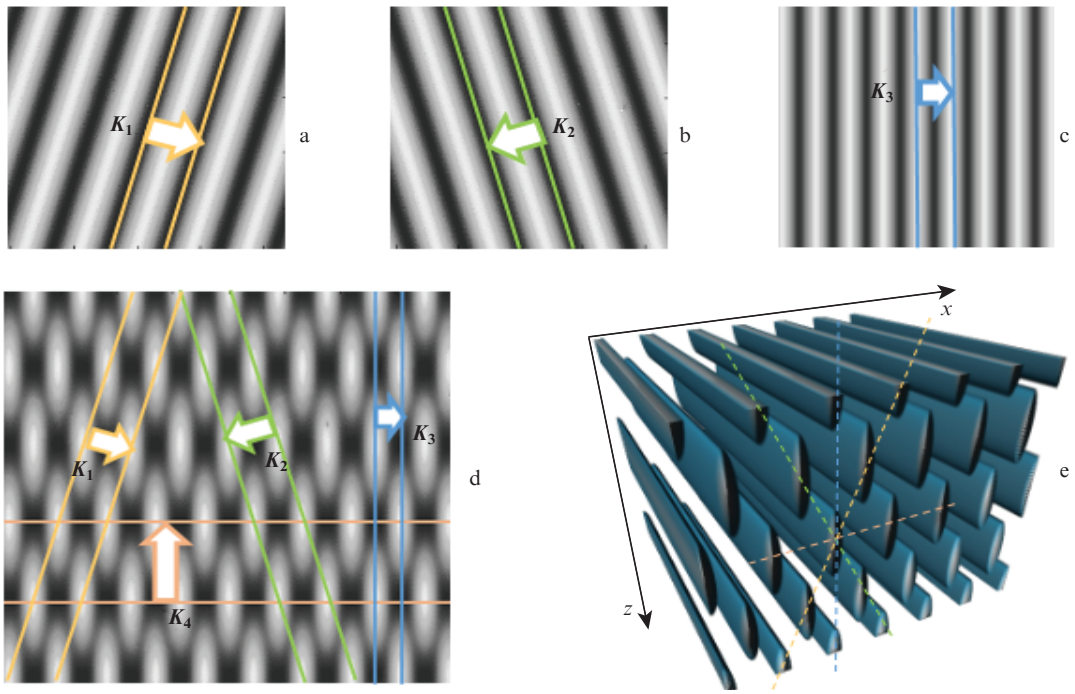

Figure 2. (Colour online) Schematic illustrating the formation of strata in a photosensitive material when optical radiation is incident on a template along the normal to it: light intensity distribution for interference between the beams of (a) the 0 and +1 orders, (b) the +1 and –1 orders and (c) the 0 and –1 orders and (d) three-beam interference; (e) image of the 3D structure.

ing the problem of optical replication. The Bragg condition for them has the form

$$\lambda = 2dn_{\text{sub}}\sin(\theta_{\text{sub}} - \gamma), \tag{2}$$

where γ is the angle between the interference planes of the Bragg grating and the normal to the surface of the photomaterial substrate; θ_{sub} is the angle of incidence of optical radiation with respect to the normal to the substrate surface in the medium; and d is the period of the 3D interference structure (future Bragg grating). The diffraction efficiency of the template ('thin' surface-relief phase grating) determines contrast in recording the entire structure in the photosensitive material. Simulation results indicate that, even at very low diffraction efficiency (within 3%), the interference fringe contrast remains above 0.6 in region II, for three-beam interference, and above 0.34 in regions I and III, for two-beam interference. It is worth noting that, upon a decrease in contrast, it is necessary to raise the minimum light intensity in the interference field. This is important in choosing exposure in order to completely utilise the dynamic range of the photosensitive material.

As an example, Table 1 presents diffraction parameters for particular interference structures calculated for the green spectral region. For recording, we used a UV laser emitting at a wavelength λ = 343 nm (in the sensitivity range of DCG). The photomask grating period d_s was 435 nm (Fig. 1). The structure was calculated for converting an input image to an output one using light with a wavelength λ_G = 520 nm. The refractive index of the material was taken to be n = 1.5. The angle of incidence of light during recording (θ_{inc} = –15°) uniquely determines all four stratum directions: 'working' direction $\boldsymbol{K}_2$ and 'parasitic' ones $\boldsymbol{K}_1$, $\boldsymbol{K}_3$ and $\boldsymbol{K}_4$ (Fig. 2).

Note that, in the above example, Bragg diffraction by parasitic gratings (structures) occurs in the IR region and has no effect on the LGP image being transmitted. Nevertheless, one should expect a decrease in diffraction efficiency in the

Table 1. Bragg diffraction parameters of recorded structures.

Grating vector	$\boldsymbol{K}_2$	$\boldsymbol{K}_1$	$\boldsymbol{K}_3$	$\boldsymbol{K}_4$
Tilt angle of strata γ	$\gamma_2 = 0.5(\theta_{-1} + \theta_0)$, 26.7°	$\gamma_1 = 0.5(\theta_0 + \theta_{+1})$, –5.3°	$\gamma_3 = 0.5(\theta_{-1} + \theta_{+1})$, 11.6°	$\gamma_4 = 90°$
Bragg grating period d	$d_2 = d_s\cos\gamma_2$, 388 nm	$d_1 = d_s\cos\gamma_1$, 433 nm	$d_3 = d_s\cos\gamma_3$, 426 nm	$d_4 = 2d_s\sin(\gamma_4 - \gamma_2)\cos\gamma_1/\sin(\gamma_2 - \gamma_1)$, 1463 nm
Bragg wavelength (2)	λ_2 = 523.5 nm	λ_1 = 1109.7 nm	λ_3 = 851.7 nm	λ_4 = 2125.0 nm
Illustration				

'working' diffraction direction and, as a consequence, an increase in the 'noise' component of the output image.

The simulation results for the multiplexed Bragg grating fabrication process are presented in Fig. 3, which shows a complex interference structure obtained by multiplexing Bragg gratings via two, five and ten sequential exposures. Mathematically, this process is additive summation of results of several exposures and superposition of several interference structures on each other. In practice, the number of multiplexes is determined by the angular selectivity of the diffraction grating produced by a certain single exposure. Under LED illumination of a finished multiplexed DOE, a wave incident on its input element at a particular angle serves the function of a reference wave involved in the formation of a single structure. An analogous principle is valid for the output DOE. By virtue of the properties of Bragg diffraction, under illumination of the input multiplexed Bragg grating diffraction occurs only from the grating in the formation of which it participated and restores only the associated object wave meeting Bragg's law.

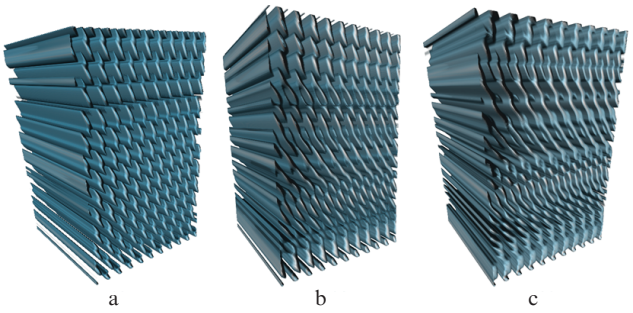

Figure 3. 3D illustration of the formation of a volume interference structure in a photosensitive material: multiplexes of (a) two sequential exposures (recording angles of 15° and 35°), (b) five sequential exposures (recording angles from 15° to 35° with 5° steps) and (c) ten sequential exposures (recording angles from 4° to 40° with 4° steps).

The dynamic range of refractive index modulation imposes certain limitations on the effective use of a recording medium in the case of multiplexing. Moreover, multiplex recording through a single photomask is associated with permissible angles of the incident beam because, in the substrate region, beams of all three diffraction orders (0, +1, and –1) should exist according to the diffraction grating equation. In the case shown in Fig. 3, a photomask with a period d_s = 396 nm interacted with UV radiation (λ = 325 nm), which limited the recording angle θ_{inc} by about 40°.

3. Experimental results

Using the optical replication method described above, we carried out a number of experiments aimed at recording multiplexed Bragg gratings in 15-μm-thick DCG layers by laser light at a wavelength λ = 405 nm. The writing beam diameter was 40 mm. To observe an image transmitted by a light guide plate with a DOE, we used a broadband light emitting diode (λ = 520 ± 15 nm). First, using angular selectivity data obtained for Bragg gratings by coupled wave theory calculations [9], we evaluated the photomask period and required angles of incidence for multiplex recording. Table 2 lists the spatial frequencies obtained for Bragg gratings in the case of multiplexing for seven sequential exposures of a photomask with a spatial frequency ν_s = 2530 lines per millimetre.

Table 2. Spatial frequency of the Bragg gratings.

Exposure no.	Grating frequency ν_2/lines mm^{-1}	Exposure no.	Grating frequency ν_2/lines mm^{-1}
1	2748	5	3100
2	2809	6	3282
3	2883	7	3757
4	2977		

An experimental sample with multiplexed Bragg gratings, fabricated in accordance with spectral and angular characteristics of an illuminator, was placed in the optical system of an augmented reality device [15]. Figure 4 shows a photograph of a monochromatic test image obtained using a light guide plate with a DOE of seven multiplexed Bragg gratings. In the background, there is an image of a mount on an optical bench. The field of view angle of the transmitted image was 2ω = 27°, and the angular selectivity of each Bragg grating in the multiplex was about 3.85°.

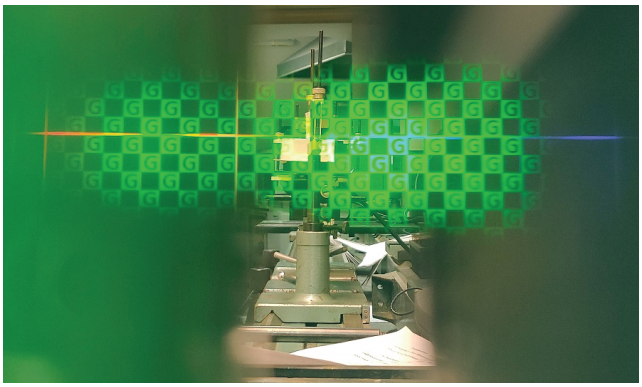

Figure 4. Monochromatic test image transmitted by a light guide plate with a DOE consisting of seven multiplexed Bragg gratings.

The described method allows one to produce light guide plates with DOEs for visual optical instruments and augmented reality devices and can be used for the fabrication of nanoelectronic components, photonic crystals, metamaterials and subwavelength structures. Of particular interest is the application of light guide plates with DOEs for the input/output of multicolour RGB images in which symbol information is spatially separated in a horizontal field of view. In such a case, additional multiplexed Bragg gratings responsible for additional wavelengths are not needed. When an image is displayed, its parts with different colours are distributed over the field in a natural manner, in accordance with the spectral properties of the multiplexed Bragg gratings (Fig. 3). The fabrication of colour augmented reality systems employing light guides with Bragg gratings requires, to a first approximation, three times as much multiplexes for recording.

Acknowledgements. This work was supported by the Russian Science Foundation (Project No. 18-79-00304).

References

1. Zhang Y., Fang F. *Precis. Eng.*, **60**, 482 (2019).

2. Syberfeldt A., Danielsson O., Gustavsson P. *IEEE Access*, **5**, 9118 (2017).
3. Draper C.T. et al. *Appl. Opt*., **58**, A251 (2019).
4. Yin K., Lee Y.H., He Z., Wu S.T. *Opt. Express*, **27**, 5814 (2019).
5. Xiao J., Liu L., Han J., Wang Y. *Opt. Commun*., **452**, 411 (2019).
6. Waldern J.D., Grant A.J., Popovich M.M. *Proc. SPIE*, **10676**, 106760G (2018).
7. Ingersoll G.B., Leger J.R. *Appl. Opt*., **54**, 6244 (2015).
8. Pimpin A., Srituravanich W. *Eng. J*., **16**, 38 (2012).
9. Kuzmin D.V. et al. *Trudy IX Mezhdunar. konf. po fotonike i informatsionnoi optike* (Proc. IX Int. Conf on Photonics and Information Optics) (Moscow: NIYaU MIFI, 2020) p. 641.
10. Vanin V.A. *Sov. J. Quantum Electron.*, **8**, 809 (1978) [*Kvantovaya Elektron.*, **5**, 1413 (1978)].
11. Campbell M. et al. *Nature*, **404**, 53 (2000).
12. Miklyaev Yu.V. et al. *Komp'yut. Opt*., **32**, 357 (2008).
13. Chanda D., Abolghasemi L., Herman P.R. *Opt. Express*, **14**, 8568 (2006).
14. Wolf A.J. et al. *Microelectron. Eng*., **98**, 293 (2012).
15. Grad Ya.A. et al. *Proc. SPIE*, **10679**, 106791W (2018).